

# Determination of the resistivity distribution along underground pipes in urban contexts using galvanic and capacitive methods

Simon Rejkjær<sup>1\*</sup>, Cécile Finco<sup>2</sup>, Cyril Schamper<sup>2</sup>, Fayçal Rejiba<sup>3</sup>,  
Alain Tabbagh<sup>2</sup>, Jesper König<sup>4</sup> and Torleif Dahlin<sup>1</sup>

<sup>1</sup>Engineering Geology, Lund University, Box 118, Lund, S-221 00, Sweden, <sup>2</sup>Sorbonne Université, UMR7619 Métis, 4 place Jussieu 75252 Paris cedex 05, France, <sup>3</sup>Normandie University, UNIROUEN, UNICAEN, CNRS, M2C, Rouen, 76000, France, and <sup>4</sup>Swedish Water Research, Ideon Science Park, Scheelevägen 15, Lund, SE-223 70, Sweden

Received April 2019, revision accepted October 2020

## ABSTRACT

Renovation of water and central heating pipelines is a very costly and time-consuming process; therefore, a way to prioritize the limited resources between different parts of the systems is very important. The risk for corrosion damage can be assessed from the resistivity of the ground, because the processes facilitating the metal oxidation also affect the resistivity. However, galvanic resistivity mapping is time consuming and work-intensive in paved areas. To determine the resistivity in the vicinity of pipes two different resistivity methods were applied: electrical resistivity tomography using galvanic coupling, and the logistically easier and rapid electrostatic measurements using capacitive coupling. The two methods were tested in a series of experiments undertaken in the province of Scania in southern Sweden with the aim to acquire a better knowledge about the electrical resistivity of the soil surrounding the heating and water distribution pipes, in order to better assess the corrosivity of the environment. From the experiments it is shown that the electrical resistivity tomography and electrostatic methods mostly give comparable results for the shallow investigated depths in focus here, where differences might be caused by different sensitivities and noise characteristics. In the case of both methods, it is shown, with the help of modelling of the different expected ground models including the pipes, that the pipes only influence the data in cases of pipes of very large diameters or those buried at a very shallow depth, even without any protective surface coating. The missing influence of the pipes on the data makes the methods very applicable for knowing the resistivity of the soil surrounding the pipes and thus evaluation of corrosion risk.

**Key words:** Near-surface, Resistivity, Site characterization.

## INTRODUCTION

Extensive networks of buried pipes for water transport and heating exist all over the world. Corrosion and leakages are common problems, so maintenance and replacement of pipes are important aspects of a functioning system. However, the replacement of pipes is a very costly process, and a

re-investment rate of 0.8% per year would be necessary to maintain the current level of conservation. With the current re-investment level in Sweden of 0.2%, it would take an estimated 500 years to change the water pipes and 350 years to change the heating pipes. This is significantly longer than the expected lifetime of the pipes, and it is therefore necessary to find a way to prioritize the limited resources and figure out where to begin (Malm *et al.*, 2011).

Corrosion of a pipe is difficult to detect precisely without uncovering long stretches of pipe and visually inspecting

\*E-mail: [simon.rejkjar@tg.lth.se](mailto:simon.rejkjar@tg.lth.se)

the state of corrosion. Several factors influence the corrosivity of the environment around the pipes such as pH, ion content and moisture content of the soil, which are also tied to lowering the resistivity of the soil. This leads to a correlation between resistivity and corrosivity as described by Roberge (2008), with low resistivity indicating a higher corrosivity and high resistivity indicating a lower corrosivity. Resistivity measurements might also show indications of missing surface protection of the pipe, which would help in risk assessments. It is also known that locations with variations in resistivity, associated with change in soil type, are often associated with corrosion problems such as clays (Roberge, 2008). A series of experiments were undertaken in the province Scania in southern Sweden with the aim to acquire a better knowledge about the electrical resistivity of the soil surrounding heating and water distribution pipes, in order to better assess the corrosivity of the environment. Hereafter the results of these experiments will be presented.

Geophysical exploration in cities is recognized as a relevant tool to better define and plan work, to reduce the extent of excavations and minimizing risks. However, surveys in urban contexts face specific difficulties that can be classified in four categories: (1) physical and regulation constraints limiting the size, location and accessibility of the measurement area, (2) the surface material (which should remain undamaged if possible), (3) the presence of numerous and potentially strong sources of electrical, electromagnetic or mechanical noise, and (4) the presence of objects or features at the surface or just beneath it disturbing measurements (they can be called 'geophysical noises'). It should also be stated that it is appropriate for the surveys to be as fast as possible to facilitate their logistics and social acceptance.

For thirty years, ground penetrating radar (GPR) has been used for pipe and cable detection; the ability of GPR to assess the water content is well established but is severely limited by penetration depth in conductive environments, which have led surveyors to study and test other techniques. For electrical resistivity investigations, the electrostatic method where both the injection and the measurements are performed by open capacitors constitute an attractive alternative method (Tabbagh *et al.*, 1993; Kuras *et al.*, 2006). It has been used with success in towns for archaeology with urban pattern recognitions (Hesse *et al.*, 2002) or ancient building studies (Dabas *et al.*, 2000; Flageul *et al.*, 2013) and civil engineering applications (Burton, 2011; Loke *et al.*, 2013).

Two independent resistivity techniques were tested in parallel: electrical resistivity tomography with its classical set up and electrodes mechanically driven into the pavement, and the

multipole version of the electrostatic technique called 'sliding carpet'. This twofold approach allows a direct comparison of speed and measurement quality in an operational context and could be used for validation and calibration to increase the reliability of the results.

## PROSPECTING TECHNIQUES AND INSTRUMENTS

### Electrical resistivity tomography

Electrical resistivity tomography (ERT) profiles were conducted using an ABEM Terrameter LS2 with an 81-electrode roll-along layout, with either 1 or 2 m electrode separation, using a multiple gradient array protocol (Dahlin and Zhou, 2006). The electrodes were inserted in the mostly paved surfaces by drilling holes slightly larger than the electrodes and adding a starch gel to decrease contact resistance as illustrated in Figure 1. The raw data of the four different examples presented here contain between 1931 and 2060 measurements depending on the number of electrodes in the line, and the transmitted current varied between 30 and 500 mA. With respect to data quality, manual inspection and culling were performed, where very few data points were removed as outliers. Inversions of the data were carried out in RES2DINV using an L1 norm robust inversion with a low vertical to horizontal flatness filter ratio (0.25) due to the expected horizontal layers (Loke *et al.*, 2003), with a cell size equal to half the electrode spacing. A depth of investigation (DOI) was estimated using the method described by Oldenburg and Li (1999) with a DOI index of 0.1. It would have been possible to use a stricter threshold, but the choice was made to keep the more standard value of 0.1 recommended by Oldenburg and Li (1999).

### Electrostatic sliding carpet

In the electrostatic method (Flageul *et al.*, 2013), capacitive electrostatic poles can be flat sheets of metal lying on the ground, and in the present version copper wire gauze was used. This solution allows each pole to be placed in pockets borne by a plastic carpet spread on the ground surface (Fig. 2). To limit the pole extents in the direction parallel to the array and integrate the signal along the perpendicular direction, poles are rectangular with the longest side perpendicular to the array. The injection poles have a  $0.4 \times 0.80 \text{ m}^2$  area, while the voltage ones have a  $0.2 \times 0.80 \text{ m}^2$  area, this allows the point-pole assumption in modelling interpretation (Uhlemann and Kuras, 2014).



**Figure 1** Sketch showing part of the ERT layout, and photo of a drilled hole with an electrode and blue starch gel (Johnson Revert Optimum®) used to reduce contact resistance.

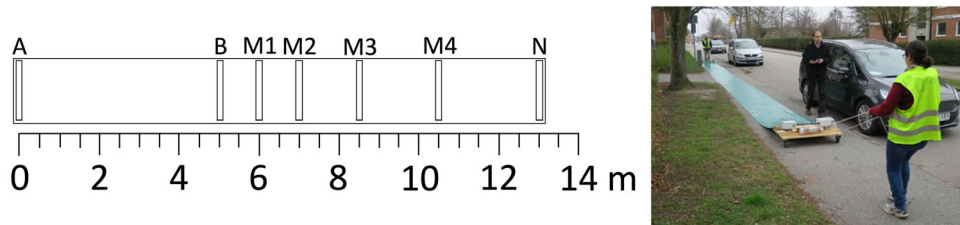


**Figure 2** Scheme of the positions of the poles and picture showing the sliding carpet in a street.

Contrary to the classical ERT, the location of each pole on the carpet is open, and after optimization tests on 3D models, a four-channel multipole array configuration was chosen and not reconfigured for the present experiment. The configuration is shown in Figure 2. When pulling the carpet, measurements can be performed ‘continuously’ on each channel with simultaneous measurements. Such a system can thus be viewed as a sliding vertical electrical sounding which provides on-the-go measurement: a 200-m long profile is measured in both directions within 10 min. The sampling distance between two successive measurements is 0.2 m, controlled by an optical counter associated with the wheels, which allows filtering to reject the outliers, avoid spatial aliasing associated with the surficial ‘geophysical noise’ and smoothing of the data. The filtering of the electrostatic measurements is performed by median filtering on a sliding window with a width equal to half the  $B M_i$  distance for each channel, and final data are recorded with a 0.5-m step in the RES2DINV format. This filtering agrees with the objective established by the pipe company: in order to identify corrosivity issues, a vertical resistivity profile averaged over the total horizontal distance is de-

fined, which would deliver the likely soil resistivity around the pipe.

Considering the expected resistivity range,  $\rho$  between 20 and 500  $\Omega\text{m}$ , the frequency,  $f = 15.6$  kHz, of the sliding carpet transmitted signal, the distance between  $B$  and  $M_4$  poles,  $L = 5.5$  m and the value,  $\mu_0$ , of the magnetic permeability of the vacuum, the induction number,  $B^2 = 2\pi f \mu_0 L^2 / \rho$ , remains lower than 0.2. Consequently, it is possible (Benderitter *et al.*, 1994; Tabbagh and Panissod, 2000) to interpret the electrostatic sliding carpet results by using DC static equations and inversion programmes, in practice here the same code as for galvanic measurements. As with the ERT, a DOI was estimated for the electrostatic profile with a standard DOI index of 0.1.

## ASSESSMENT OF A PIPE EFFECT IN RESISTIVITY SURVEYING

The experiment goal is the determination of the electrical resistivity of the terrain around a metal pipe by measuring on the ground surface with arrays laid out centred above the pipe. One must first assess the possible influence of the pipe itself on

the measured apparent resistivity. In other words, one needs either to know the pipe diameter and the depth under which a negligible influence can be assumed or to quantify the response of the pipe.

The difficulty of the very high resistivity contrast between the metal pipe and the surrounding terrain must be overcome to successfully model this situation. In DC resistivity, metallic feature responses differ from that of the electromagnetic case (Thiesson *et al.*, 2018) where the induction effect is huge and increases with the metal conductivity. Here, if the pipe is protected by a painted or a plastic isolating cover, it corresponds to a resistivity contrast,  $(\rho_{\text{pipe}} + \rho)/(\rho_{\text{pipe}} - \rho)$ , tending towards 1, while the contrast will tend towards  $-1$  if the metal is bare or inserted in a concrete gang. With such contrasts, it is not easy to use a purely numerical method as those used in the inversion software where the metal itself would have to be very finely meshed. The most relevant method is an integral equation approach where the presence of the 3D metal surface is equivalent to a charge density over it (Alfano, 1959; Spahos, 1979; Li and Oldenburg, 1991; Boulanger and Chouteau, 2005). Electromagnetic induction is not considered in this modelling approach.

We illustrate the possible influence of the pipe by considering the synthetic responses that would be obtained with the sliding carpet pole locations, but the responses for a classical electrical resistivity tomography (ERT) set-up would be qualitatively similar. The case assumes an unprotected metallic pipe since an insulating cover will decrease the effects.

In the case of a profile carried out parallel to a buried uncovered metallic pipe, the results have a big dependency on the offset between the pipe and the profile. In Figure 3, the results from the four channels of the sliding carpet are shown at different lateral distances parallel to a 0.4-m diameter bare steel pipe, buried at a depth of 1 m (from its centre). The surrounding terrain and the steel pipe have resistivity of 100  $\Omega\text{m}$  and  $1.7 \cdot 10^{-7} \Omega\text{m}$ , respectively (cast iron with  $10^{-6} \Omega\text{m}$  would not give a significantly different contrast). It can be observed that the pipe corresponds to a clear conductive anomaly in channels 1 and 2, whereas to an oscillating one in channels 3 and 4. The anomalies remain limited in amplitude to a maximum of 20% for channel 1 and to less than 10% for channel 4. In Figure 4, a resistivity section centred along the uncovered metallic pipe is shown. A direct interpretation of such a pseudo-section would suggest the existence of a superficial conductive layer. If the pipe is isolated by a protecting layer, it appears as a small resistive target with a maximum apparent resistivity of 105  $\Omega\text{m}$  (on channel 1), which will not

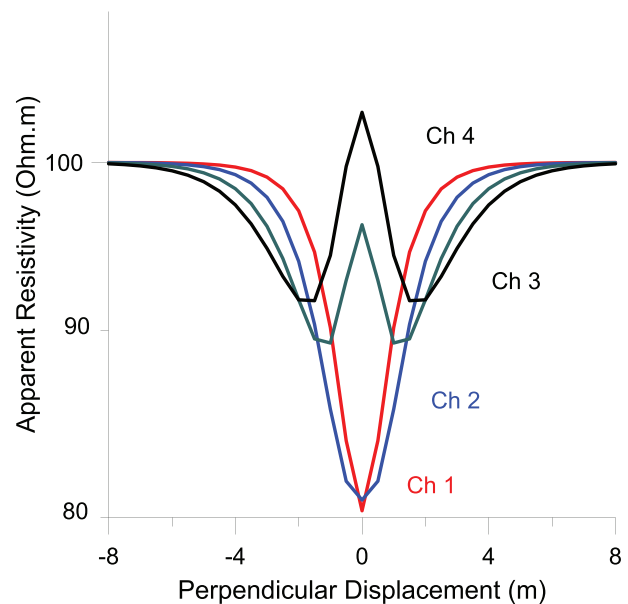


Figure 3 Apparent resistivity for the four channels, as a function of the perpendicular offset between the parallel pipe and sliding carpet (0.4 m diameter steel pipe centred at 1 m depth).

be identified when conducting *in situ* measurements. For this simple case, one can remark that the influence of the pipe is not so important: 0.4 m is a rather big diameter and  $h = 1.5$  m would be more usual than  $h = 1$  m. However, for bare pipes it is interesting to illustrate the role of the diameter at a given centre depth and the role of the depth for a given diameter. In Figure 5(a), the evolution of the ratio of the measured apparent resistivity to the homogeneous ground resistivity (100  $\Omega\text{m}$ ) is presented for a 0.4-m diameter pipe when the depth of its centre varies from 0.8 m to 1.6 m. In Figure 5(b), the same ratio is presented for a variation of the pipe diameter between 0.2 and 1 m when the depth of the centre equals 1.2 m. With the exceptions of large pipes and shallow depths, the ratio remains close to 1.

## EFFECT OF THE ARRAY DISSIMILARITIES

Having established that the effect of a pipe would be limited when using the resistivity method, it can be expected that, in contrast with the electromagnetic induction methods, the determination of the ground resistivity around a buried pipe is possible. The two independent techniques are then implemented to compare their respective results and also to evaluate their operability in an urban environment. As the electrostatic method can be interpreted under static assumption, the use of the two techniques only differs by two aspects: (1)

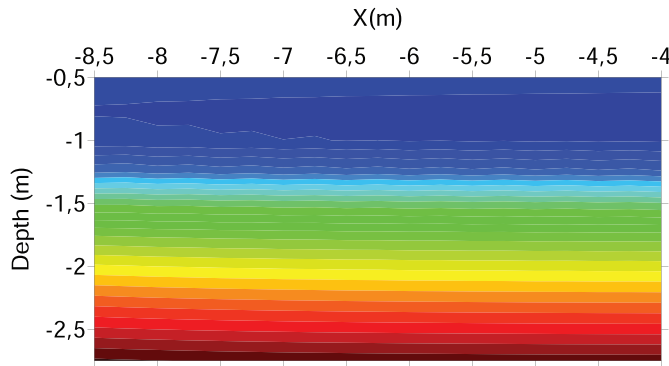


Figure 4 Apparent resistivity pseudo-section, centred above and parallel to a pipe, where the channel 1 measurements are referred to  $z = 0.5$  m depth, the channel 2 measurements to  $z = 1$  m depth, the channel 3 measurements to  $z = 1.75$  m depth and the channel 4 measurements to  $z = 2.75$  m (0.4 m diameter steel pipe located at 1 m depth; the  $x$  values are referred to the position of A pole).

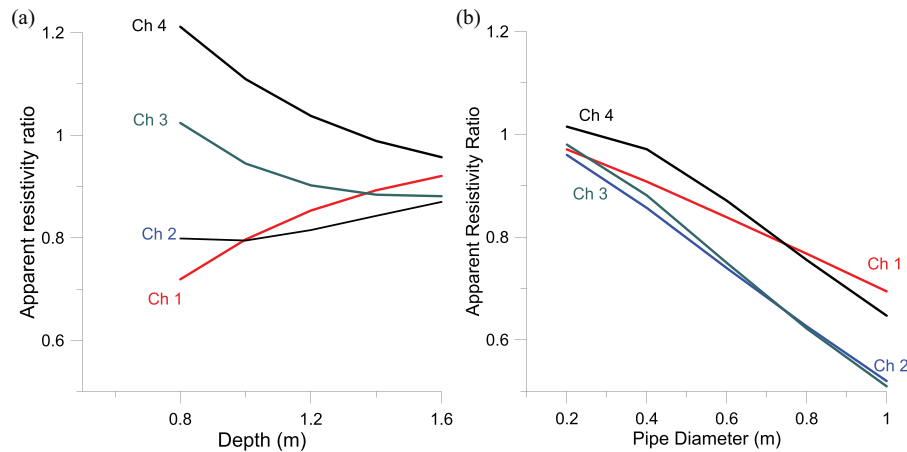


Figure 5 (a) The ratio of the measured apparent resistivity to the homogeneous ground resistivity ( $100 \Omega\text{m}$ ) as a function of the depth of the centre at which the 0.4 m diameter pipe is buried. (b) The ratio as a function of the diameter of a pipe buried with the centre at a depth of 1.2 m.

the electrodes or pole layouts: one is the classical regularly spaced electrical resistivity tomography (ERT) positioning and the other a specific pole layout defined in another context, not *a priori* optimized for this experiment and only allowing four different depths of investigation, (2) while the ERT electrodes are driven into the pavement (and may cross it), the electrostatic poles are lying over this layer which consequently may modify the apparent resistivity. These two aspects have both advantages and drawbacks: the sliding carpet is limited in terms of depths of investigation, the greater distance between electrodes being 13 m. However, the 0.2-m measurement step together with the pole area offers the ability to eliminate the effect of possible disturbing surficial objects (by means of moving median filtering). The ERT system can be spread out along 50, 100 m or more, which allows a substantial depth of investigation, but the 1 m electrode spacing, in this given case, may generate spatial aliasing. Consequently, it is wise prior to processing field data to grasp the difference in the detection ability of the two techniques with synthetic cases.

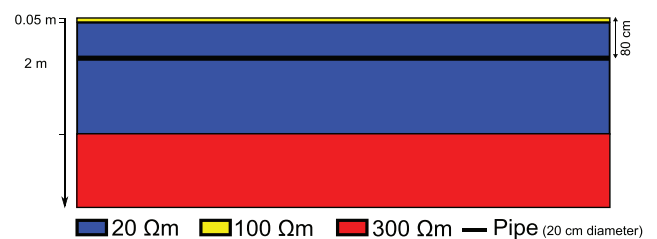
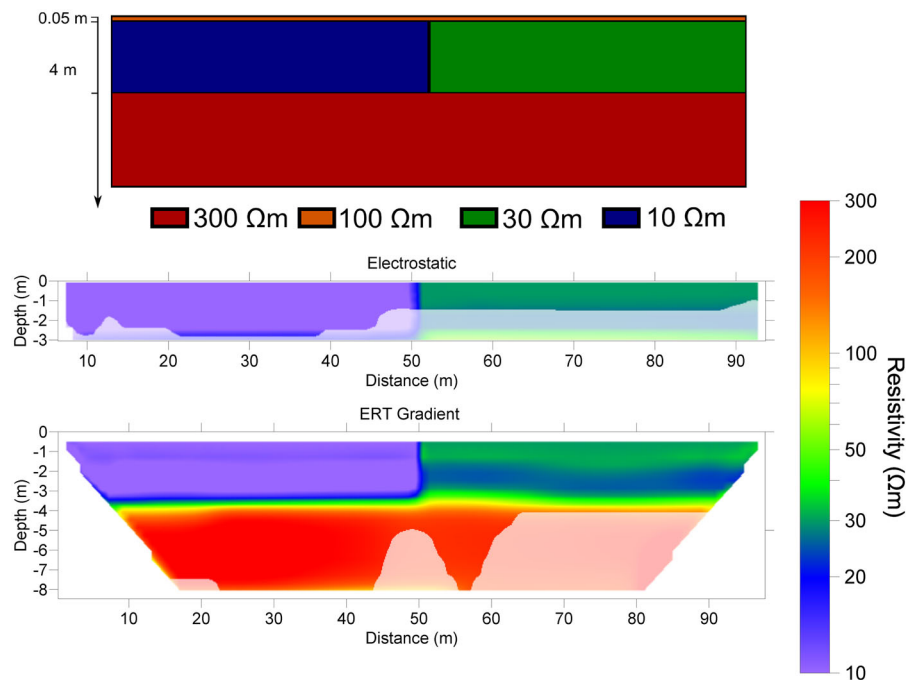


Figure 6 Sketch showing the pipe inside the second layer of a three-layer terrain.

A three-layer model with the pipe located in the second, conductive, layer is thus considered as illustrated in Figure 6. The pipe is assumed to be parallel to the arrays (also to the street direction) and in the same vertical plane; hence, the pipe corresponds to an elongated feature parallel to the current injection. Assuming that it has protective coating, it would constitute a relatively small resistive feature. Another case with lateral variation in the second layer was also considered (Fig. 7). In each case, the acquisition set-up used in the



**Figure 7** Sketch of a three-layer model with a lateral variability in the conductive second layer (top). Result of the forward modelling and inversion with both the electrostatic sliding carpet and the ERT gradient array (respectively middle and bottom). Regions with DOI indexes exceeding 0.1 are shaded in white.

simulations corresponds to the layout used during the field experiment. The interpretation is done using the same RES2DINV software with L1 norm, as for the experimental data. Since all examples from the field experiment present a conductive layer, several synthetic models are considered to assess the abilities of both arrays and of the inversion procedure to (1) clarify the impact of the presence of the pipe in a three-layer context by comparing in each case the results with pipe and without pipe, (2) assess the possible part of superficial resistive layer corresponding to the pavement, (3) highlight the presence of a deep resistive layer below the conducting one, in order to determine the limit in depth of the conducting layer and (4) assess the sensitivity of each array to lateral variations. Considering this last point is important, since a lateral resistivity change along a pipe may significantly increase the corrosion risk, and it is thus of value to locate resistivity changes as precisely as possible.

A three-layer model is first considered with a superficial layer of 100  $\Omega\text{m}$  resistivity and 0.05 m thickness covering a conductive layer of 20  $\Omega\text{m}$  and 2 m thickness followed by a deep layer of 300  $\Omega\text{m}$  resistivity. In the second layer, a large pipe with the radius of 0.10 m is centred at the depth of 0.8 m. The calculation of the apparent resistivity along

a profile above the pipe is achieved using the integral equation approach. The apparent resistivity values obtained with both arrays and the interpreted resistivity values obtained after RES2DINV inversion are presented in Tables 1 and 2. For the apparent resistivity, the increase of the terrain thickness taken into account by the successive quadrupoles is expressed by the corresponding geometrical coefficient  $K$  (defined by  $\rho_a = K (\Delta V/I)$ ). It appears that for the sliding carpet, as well as for the multiple gradient array ERT, the difference in apparent resistivity is very limited: the pipe does not significantly change the resistivity distribution as a function of depth. The resistive third layer is well resolved by the ERT but only sensed by the sliding carpet, in particular with the pipe as its resistivity is overestimated.

When the superficial layer is not considered in the ERT, thus with a two-layer model, a conductive 20  $\Omega\text{m}$  and 2.05 m thick above the 300  $\Omega\text{m}$  resistive, both the apparent resistivity and interpreted values are slightly modified as presented in Table 3.

The changes in resistivity presented in Tables 4 and 5 correspond to the situation where the thickness of the conductive second layer is increased from 2 m to 4 m. Again the presence of the pipe does not significantly change the vertical

**Table 1** Comparison between the three-layer terrain without and with pipe at 0.8 m depth: Sliding carpet ( $\rho_1 = 100 \Omega\text{m}$ ,  $e_1 = 0.05 \text{ m}$ ,  $\rho_2 = 20 \Omega\text{m}$ ,  $e_2 = 2 \text{ m}$ ,  $\rho_3 = 300 \Omega\text{m}$ )

Sliding carpet Apparent resistivity ( $\Omega\text{m}$ )			Sliding carpet RES2DINV inverted resistivity ( $\Omega\text{m}$ )		
K (m)	Without pipe	With pipe	Depth (m)	Without pipe	With pipe
8.00	22.56	21.08	0.33	20.08	19.39
20.33	26.51	25.26	1.03	18.04	14.51
52.36	32.94	32.95	1.79	29.10	32.63
163.19	40.14	41.19	2.64	246.17	410.71

**Table 2** Comparison between the three-layer terrain without and with pipe at 0.8 m depth: multiple gradient array ERT ( $\rho_1 = 100 \Omega\text{m}$ ,  $e_1 = 0.05 \text{ m}$ ,  $\rho_2 = 20 \Omega\text{m}$ ,  $e_2 = 2 \text{ m}$ ,  $\rho_3 = 300 \Omega\text{m}$ )

ERT Apparent resistivity ( $\Omega\text{m}$ )			ERT RES2DINV inverted resistivity ( $\Omega\text{m}$ )		
K (m)	Without pipe	With pipe	Depth (m)	Without pipe	With pipe
12.23	22.89	21.03	0.25	20.52	21.62
24.45	30.56	29.47	0.81	19.32	12.81
58.66	37.46	36.92	1.52	19.13	25.44
117.32	65.54	69.51	2.39	139.07	265.78
234.65	109.60	110.48	3.49	318.00	304.10

distribution of the resistivity. In that case, contrary to multiple gradient array ERT, the sliding carpet is quasi-insensitive to the presence of the resistive deep layer.

The results of the simulations with lateral variations within the depth range expected for the pipes of the electrical resistivity in the conductive layer are presented in Figure 7. It appears that both the ERT and the electrostatic were able to precisely resolve the lateral variation introduced in the model. As expected, the depth of investigation (DOI) reached on the ERT profile is deeper, at least 4 m deep, than the electrostatic profile where DOI reaches at most 3 m. It can be noted that for both methods, the DOI is more impor-

tant on the more conductive half of the model (left side in Fig. 7).

## RESULTS AND INTERPRETATION

When looking at the profiles, one first observes rapid lateral changes, that is, a significant geophysical noise. Its high spatial frequency character implies that it must result from superficial resistivity changes in relation with the first layer heterogeneity. These variations are smoothed out in the electrostatic measurements due to the filtering. The electrical resistivity

**Table 3** Comparison between the two layers terrain without and with pipe at 0.8 m depth: multiple gradient array ERT ( $\rho_1 = 20 \Omega\text{m}$ ,  $e_1 = 2.05 \text{ m}$ ,  $\rho_2 = 300 \Omega\text{m}$ )

ERT Apparent resistivity ( $\Omega\text{m}$ )			ERT RES2DINV inverted resistivity ( $\Omega\text{m}$ )		
K (m)	Without pipe	With pipe	Depth (m)	Without pipe	With pipe
12.23	22.70	20.94	0.25	20.41	20.85
24.45	30.18	28.74	0.81	19.25	13.54
58.66	36.89	36.22	1.52	18.89	23.40
117.32	64.51	68.04	2.39	119.43	270.35
234.65	108.12	108.98	3.49	324.97	337.61

**Table 4** Comparison between the three-layer terrain without and with pipe at 0.8 m depth when the conductive layer is thicker (4 m in place of 2 m): sliding carpet

Sliding carpet Apparent resistivity ( $\Omega\cdot\text{m}$ )			Sliding carpet RES2DINV inverted resistivity ( $\Omega\cdot\text{m}$ )		
K (m)	Without pipe	With pipe	Depth (m)	Without pipe	With pipe
8.00	19.86	18.75	0.33	21.00	19.02
20.33	20.00	19.96	1.03	17.11	16.20
52.36	20.91	22.36	1.79	16.69	17.99
163.19	22.85	24.29	2.64	31.94	39.61

tomography (ERT) profiles include data at a significantly bigger depth than the capacitive resistivity ones. Since the area of interest when looking at buried pipes is only the top 3 m, this will be the focus from here.

For the different locations, soil maps provided by the Swedish Geological Survey (SGU, 2019) were consulted for a basic understanding of the geological setting in the areas.

#### Slammarpsvägen (Förslöv)

The geological setting at the location in Förslöv is mostly glacial sediments. From the soil map, it was found that the profile should be mainly glacial till consisting of clay. From this information, it is expected that the top layers consist of clay till or coarser fill material added when the pipe was installed.

In this first example, Figure 8, from Slammarpsvägen in Förslöv, the ERT results show a resistive top layer (above 200  $\Omega\text{m}$ ) with a thickness around 0.8 m followed by a layer with a lower (50–100  $\Omega\text{m}$ ) but highly laterally varying resistivity. The results from the electrostatic method show somewhat similar results to the ERT with a resistive top layer followed by a layer of lower resistivity, but the top layer is thinner, and the second layer has less lateral resistivity variations in accordance with the applied filtering. The two methods show somewhat

significant differences in especially two sections. The first section being 10–20 m, where the resistivity of the top layer is lower and its thickness larger for ERT. The second layer shows different anomalies. The anomalies are on the edge of the depth of investigation (DOI), so can at least partly be explained by the loss of sensitivity. The difference in the top layer could be a combination of the smoothing performed on the capacitive data, and of the 1-m ERT electrode spacing not being able to resolve a thin resistive layer properly, which implies the layer to appear thicker and less resistive in the inversion results. The second section where the two models differ is between 50 and 90 m, where the capacitive method shows a third resistive layer, close again to the DOI limit.

In general, the average vertical resistivity profile can be described by a top layer with a resistivity above 200  $\Omega\text{m}$  and a thickness around 0.8 m lying over a second 50  $\Omega\text{m}$  layer. However, this layer in this case exhibits low-frequency lateral changes in resistivity which at some places can reach up to 300  $\Omega\text{m}$  but can also reach down to the [30–50]  $\Omega\text{m}$  interval. When considering a 0.06-m diameter steel pipe located at 1.6 m depth (data given by the company), one can conclude that the pipe lies in the second layer and due to the highly varying resistivity of this layer the corrosion risk is highly variable along the explored horizontal distance. For the

**Table 5** Comparison between the three-layer terrain without and with pipe at 0.8 m depth when the conductive layer is thicker (4 m in place of 2 m): multiple gradient array ERT  $\rho_1 = 100 \Omega\text{m}$ ,  $e_1 = 0.05 \text{ m}$ ,  $\rho_2 = 20 \Omega\text{m}$ ,  $e_2 = 4 \text{ m}$ ,  $\rho_3 = 300 \Omega\text{m}$ 

ERT Apparent resistivity ( $\Omega\cdot\text{m}$ )			ERT RES2DINV inverted resistivity ( $\Omega\cdot\text{m}$ )		
K (m)	Without pipe	With pipe	Depth (m)	Without pipe	With pipe
12.23	20.70	19.14	0.25	19.86	19.51
24.45	22.77	22.17	0.81	21.03	15.52
58.66	24.41	24.62	1.52	18.75	24.19
117.32	37.24	39.57	3.49	21.32	22.49
234.65	65.15	65.48	4.87	203.94	288.90

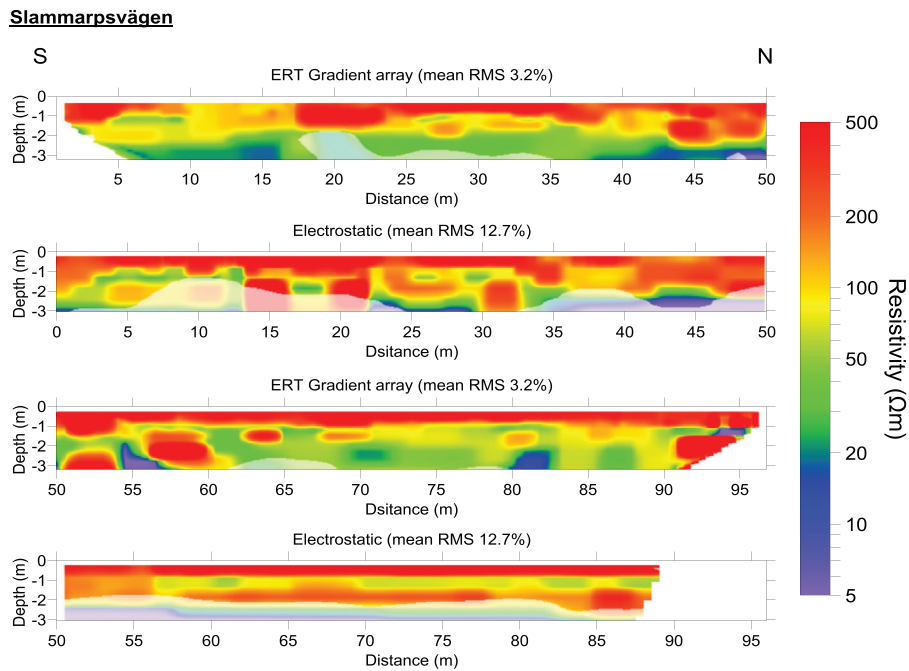


**Figure 8** Slammarpsvägen (Förslöv): ERT inversion results and electrostatic inversion results. Regions with DOI indexes exceeding 0.1 are shaded in white.

electrostatic measurements, the simulated measurement profile with a 200  $\Omega\text{m}$  first layer of 0.8 m thickness above a 50  $\Omega\text{m}$  substratum gives the same results either in the absence of pipe or with the pipe present (within a 2% limit), one can thus conclude that the resistivity of the pipe is not the cause of the effects seen in the inversions, because the pipe is too slim and too deep to be able to affect the surface measurements. The best explanation of the drop in resistivity is that the volumes around the pipe were not filled with a coarse material but with the clay till material found in the area.

#### Stampgatan North (Helsingborg)

The geological setting found from the soil maps for Helsingborg is sandy till. It is therefore expected for the Stampgatan site that sandy sediments or coarse fill materials were added when the pipe was installed.

In this second example, Figure 9, from Stampgatan in Helsingborg, the electrical resistivity tomography (ERT) again shows a resistive top layer (above 130  $\Omega\text{m}$ ), this time with a thickness of up to 1.5 m, and followed by a layer of significantly lower resistivity (as low as 10  $\Omega\text{m}$ ). The electrostatic carpet shows very similar results to the ERT again with a bit thinner top layer and less lateral variation, which can be ex-

plained by the shallow resolution and filtering of the electrostatic carpet.

The lower resistivity of the second layer can be explained by the fact that the measurements took place on the tiled pavement where runoff water can relatively easily infiltrate between the tiles, as opposed to asphalt. However, here in the second layer, again laterally variable, the interpreted resistivity can reach values as low as 10  $\Omega\text{m}$ . Such values normally correspond to massive clay or mineralized water pockets which are not what is expected from the soil maps, unless considering local accumulations of the salt spilled during winter. It is thus wise to examine in more details a possible role of the pipe itself or of a metallic wire net protecting the pipe. If we consider a two-layer model, with  $\rho_1 = 200 \Omega\text{m}$ ,  $e_1 = 1.2 \text{ m}$  and  $\rho_2 = 50 \Omega\text{m}$ , the apparent resistivity measurements for the four channels would be 150, 107, 74.7 and 60.7  $\Omega\text{m}$ . The results including a 0.15-m diameter water pipe at 1.6 m depth are not different and cannot explain the interpreted resistivity values, lower than 10  $\Omega\text{m}$ . Even with a 0.2-m diameter pipe centred at 1.3 m depth, the reduction of the apparent resistivity at the surface does not overpass 2%. A flat metallic wire netting, at 1.3 m, just below the first layer does not reduce the interpreted resistivity below 40  $\Omega\text{m}$ . With neither the inclusion of metallic objects in the subsurface or the local sediments explaining the

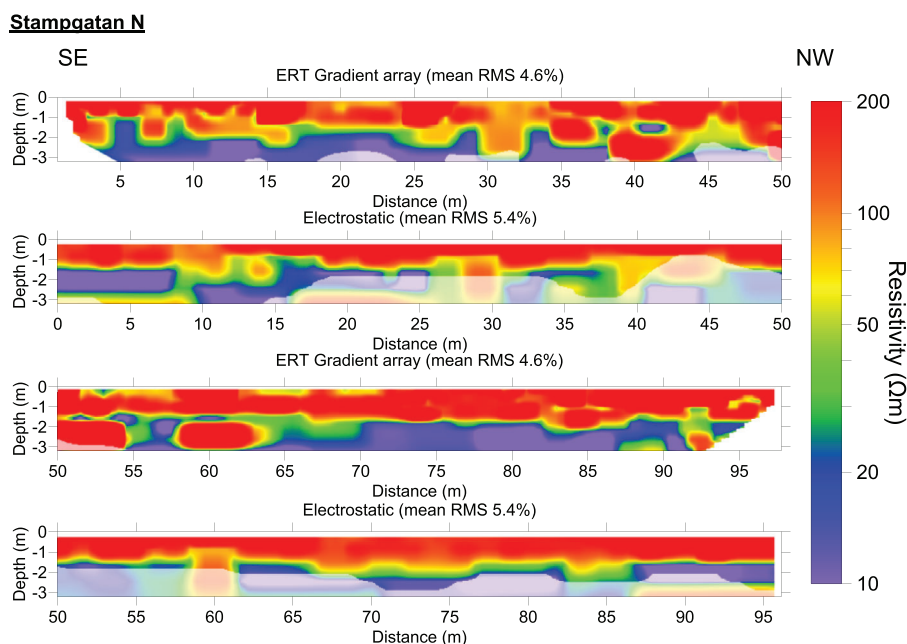


**Figure 9** Stampgatan N (Helsingborg): ERT inversion results and electrostatic inversion results. Regions with DOI indexes exceeding 0.1 are shaded in white.

low resistivity, the cause must be something different, which for example could be the accumulation of salt from the roads.

### Trastvägen (Lund)

For this location, the expected geological setting, from the soil maps, is fine clay till, so this is what is expected in combination with coarse fill material used to fill around the pipe.

In this third example, Figure 10, from Trastvägen in Lund, the ERT again shows a resistive top layer followed by a conductive layer (below 26  $\Omega\text{m}$ ), but in this case the resistive top layer has a significantly lower resistivity with much more lateral variation (40–320  $\Omega\text{m}$ ). The electrostatic method shows a thin resistive top layer (above 92  $\Omega\text{m}$ ) followed by a thin low resistivity layer (below 26  $\Omega\text{m}$ ), and a high resistivity third layer. The presence of this third layer is the main discrepancy between the two arrays. It might result from a lateral effect, but as we only have one profile and not a map to support or disprove this hypothesis. Another possible explanation lies in the difference in actual depth of investigation relative to the different array layout as discussed for the synthetic model results (Fig. 7). As seen in both cases, the DOI of the capacitive method is just below or above the top of the resistive layer. It should furthermore be kept in mind that the residuals are rather high for both methods, especially the capacitive method, which is indicative of noise or influence from 3D

structures in the data and associated difficulties to fit the data to a model in the inversion. The differences in the top layer between the two methods can have several explanations. First, the ERT at Trastvägen was measured with a 2-m electrode spacing, which decreases the resolution of the top layer significantly, so a thin top layer might not be resolved properly and end up showing as a thicker layer with lower resistivity. Second, the lateral filtering of the capacitive data set probably makes the top layer look more consistent with less lateral variations than might be in reality.

In this street, the profile has been carried out along two large heat distribution pipes (250 and 125 mm in diameter) buried at a shallower depth (0.8 m) which may explain the low resistivity values. When considering a 400  $\Omega\text{m}$  resistive and 0.2 m thick first layer above a uniform 80  $\Omega\text{m}$  layer, the presence of two pipes at 0.8 m depth significantly decreases the second layer resistivity values to around 60  $\Omega\text{m}$ , but not down to 20  $\Omega\text{m}$ .

### Karl X Gustavs Gata (Helsingborg)

In the last location, the geological setting is very similar to Stampgatan with the soil map showing sandy till and is therefore expected in combination with coarse fill material.

The results, Figure 11, from Karl X Gustav gata in Helsingborg, show two different resistivity distributions, one

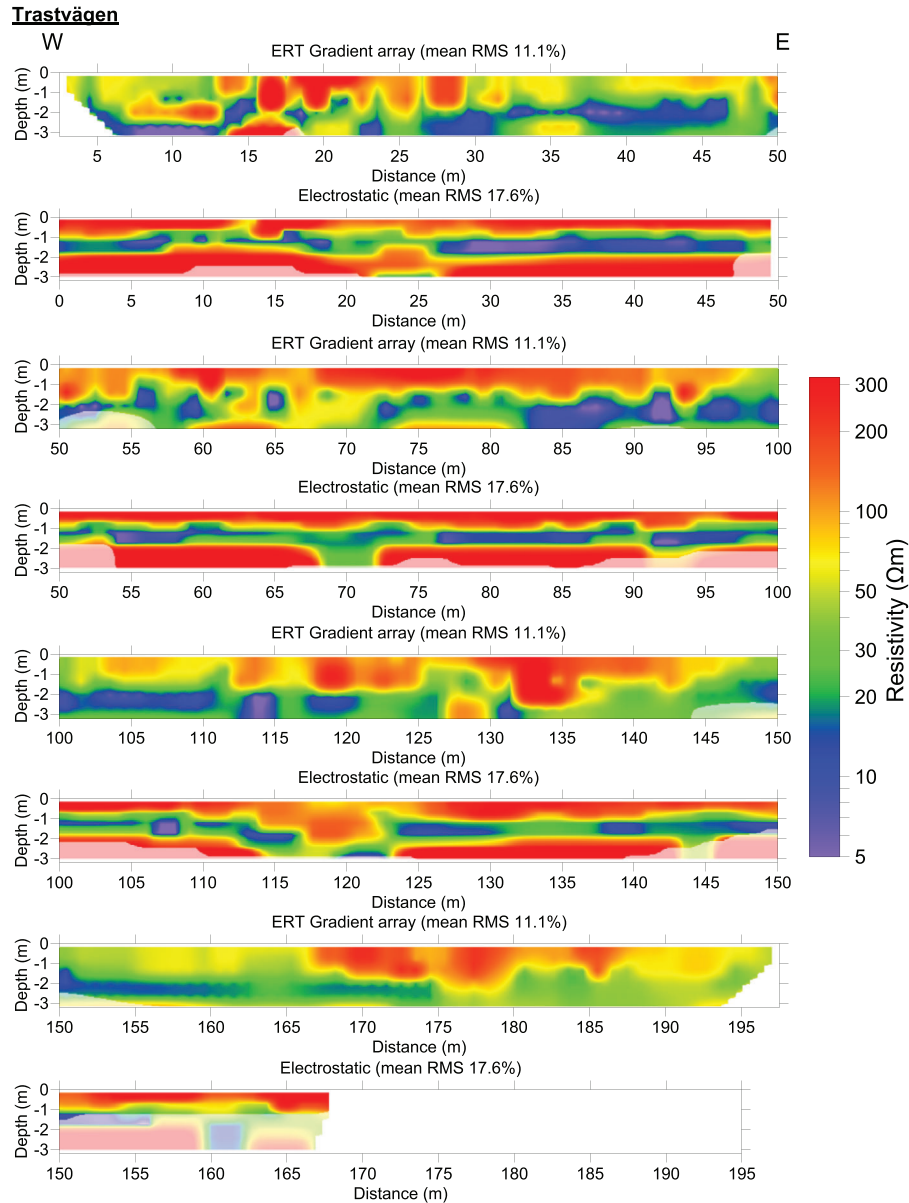


**Figure 10** Trastvägen (Lund): ERT inversion results and electrostatic inversion results. In this street, two large heat distribution pipes (250 and 125 mm in diameter) are buried at a shallow depth (0.8 m). Regions with DOI indexes exceeding 0.1 are shaded in white.

at each end of the profile. For the ERT model, the southern part of the profile shows a quite thin top layer (less than 0.8 m) with a low resistivity range (20–130  $\Omega\text{m}$ ) compared with previous examples. In the northern part of the profile, the resistive top layer extends much deeper and has a higher resistivity (above 200  $\Omega\text{m}$ ). In general, the ERT model shows a lot of lateral variations within both the resistive top layer and the more conductive second layer. The electrostatic model shows similar results to the ERT data with the southern end of the

profile having a thin resistive top layer (above 320  $\Omega\text{m}$ ) on top of a conductive second layer (below 20  $\Omega\text{m}$ ) and the northern part of the profile having the resistive top layer (above 200  $\Omega\text{m}$ ) extending much deeper with nearly no indication of a conductive layer. This example also shows the largest difference between the two methods with the ERT giving significantly lower resistivity of the top layer in the southern part of the profile compared with the electrostatic method. This difference could be due to the thin top layer, which might not be

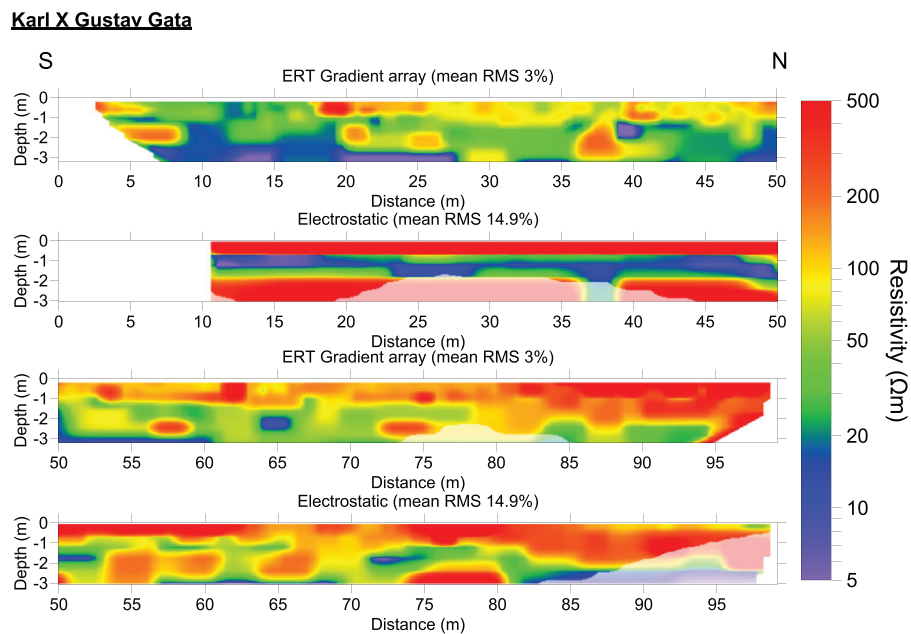


**Figure 11** Karl X Gustav gata (Helsingborg): ERT inversion results and electrostatic inversion results. Regions with DOI indexes exceeding 0.1 are shaded in white.

possible to resolve with either of the methods. The capacitive resistivity profile also indicates a third high resistive layer at the bottom edge, while there are only very few indications of this layer in the ERT model. There are some indications in the ERT model, for example, between 20 and 25 m and around 40 m along the profile. The significant difference could be ex-

plained by the 2-m inter-electrode distance of the ERT, but it is also close to the depth of investigation of the electrostatic carpet. This might cause the inversion to overestimate the resistivity due to the very low resistivity layer above as well as the higher resistivity below. Furthermore, the residuals are rather high for the capacitive method, which means

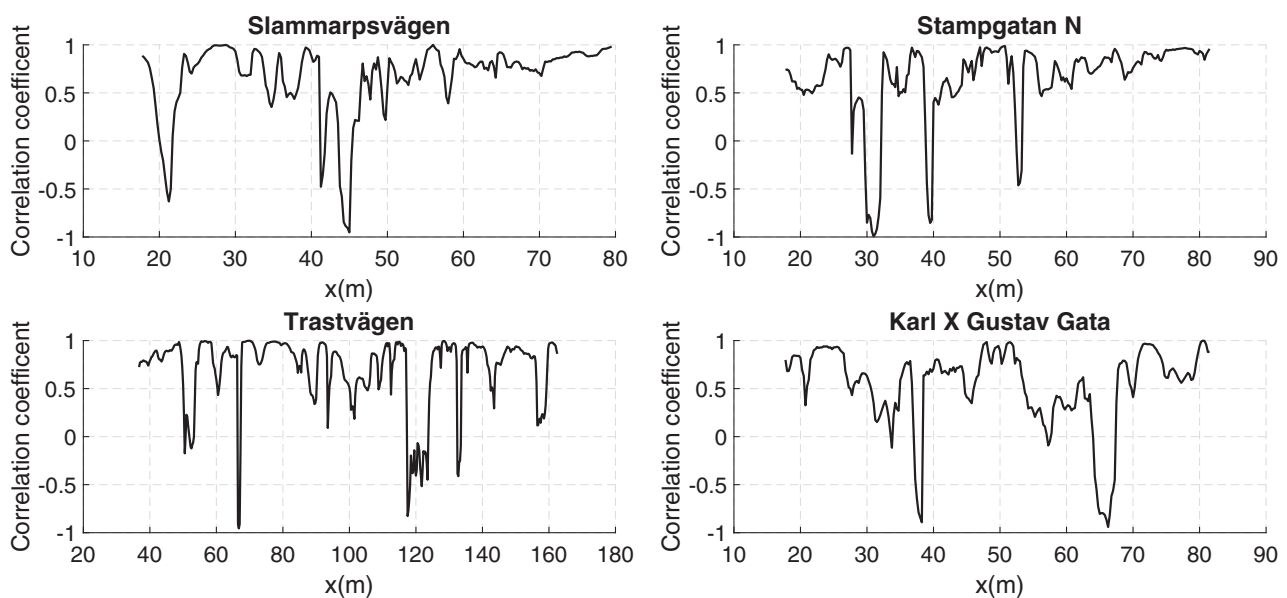


**Figure 12** Correlation coefficient over the first 2 metres along the profiles between ERT and electrostatic inversion results.



**Figure 13** Picture taken of the pipes and cables in the subsurface during the excavation at Trastvägen (Lund). The photo shows several central heating distribution pipes, electrical, internet and telephone cables.

difficulties to fit the data to a model in the inversion, which might explain the discrepancies in the southern part.

At the southern part of the profile, the results show a high resistivity top layer with a thickness up to 0.8 m and a second layer with a low resistivity. The presence of a 0.17-m diameter

pipe buried at a depth of 1.5–2 m cannot explain such a low resistivity (below 20  $\Omega\text{m}$ ), nor can the sandy till in the area. Some other influence such as salt accumulation must be considered. In the northern part of the profile, the high resistivity layer extends all the way to a depth of more than 2 m and is

more in consistency with what is expected for the area with the sandy till.

## DISCUSSION

When looking at all the combined results, the models interpreted from the electrical resistivity tomography (ERT) data and the electrostatic data are similar along much of the lines, but there are also significant differences that need to be explained. The results differ mostly in the topmost layer and its rapid lateral variations, and in that the electrostatic method in some cases indicate higher resistivity at the bottom of the inverted section. The differences in the surficial lateral variations can be explained by the pole surface and by the fact that the electrostatic data have been laterally filtered while no anti-aliasing filtering has been applied to the ERT data. The differences in the top layer can be attributed to the relatively large electrode spacing of the ERT compared with the depth-interval studied: the ERT does not have a very high data density in the first metre or so. While the electrode spacing of the 'sliding carpet' is not smaller than the ERT, this limitation is partly overcome by the much denser measurements, every 20 cm, and therefore this higher lateral sampling limit the risk of aliasing. The increase in resistivity at the bottom of the inverted sections from the electrostatic data might be explained by a shallower depth of investigation compared with the ERT. Furthermore, in a couple of cases, discrepancies might be explained by influence in the data by 3D structure or noise, as suggested by rather high residuals for the inverted models.

Correlation analysis can be made along the profiles to illustrate the parts which are correlated or un-correlated. This is illustrated in Figure 12 with the correlation estimated over the first 2 metres. Despite the remaining oscillations with low correlation coefficients (or anti-correlated values) due to the different inversion grids, acquisition geometries, field acquisition hazards, and non-exactly similar pre-processing, correlation coefficient is globally above 0.5 and, in several areas, close to 1.

In the different examples presented here, it is rare that the pipes are either large enough or buried shallow enough to give rise to any significant response, given that the pipes are coated with an electrically insulating layer. While most of the data have a drop in the resistivity for the second layer where we expect the pipes to be located, the responses of both methods are not explained by the inclusion of a pipe in a similar synthetic model and must be explained by some other effects such as a clay layer, accumulation of road salts, or the presence of other metallic features. The subsurface is never as simple as

the models used in the modelling and in reality, there are often a lot of different cables and pipes buried under the street, and these might also influence the results. An example can be seen in Figure 13, which is a picture taken during the excavation of the pipes at Trastvågen where all the cables and pipes above the investigated pipe are visible. The only pipes large enough and buried shallow enough to explain the resistivity drop in the model are two large heat distribution pipes buried at a shallow depth, and only if they had no protective coating. None of these pipe types would be detected by ERT if the coating is intact. During excavation, all the pipes were found to be in perfect condition, with the exception for some minor surface damages at Trastvågen between the approximate distances 78 m and 147 m along the profile, but it is not significant enough to cause any extra response.

Even though it is not possible to detect the pipe in the measurements, the data can still be used for the evaluation of the stretches of pipes, and on the contrary, it is an advantage as the resulting resistivity can be expected to reflect the resistivity of the formation around the pipe. Since the resistivity is correlated with the corrosivity (Roberge, 2008), the vulnerability of the pipes can be evaluated, for example, as a mean or median resistivity (corrosivity) for the specified depth where the pipe is buried, and used by the pipe owners for risk assessment.

## CONCLUSIONS

Resistivity mapping is useful for corrosion risk assessment of metal pipe networks. Since the pipe networks are very extensive and electrical resistivity tomography (ERT) is labour intensive, the technique is not ideal in this application, especially in paved areas where providing galvanic contact requires significant efforts and is destructive. In this context, the capacitive, or electrostatic, technique appears as a very attractive alternative.

Direct comparison between ERT and 'sliding carpet' results shows a generally good coherence, although there are differences that might be caused e.g. by different sensitivities and noise characteristics. This confirms the good applicability and potential usefulness of the second solution for in-town measurements due to its easy, non-destructive implementation and speed, even when considering its limited vertical resolution and possible problematic inversion results at this limit.

The very low resistivity interpreted in several profiles is never fully explained by the inclusion of a pipe affecting the resistivity and must, therefore, be explained by effects caused by the material surrounding the pipe. This difficulty clearly suggests that the underground can be more complicated than

a pipe embedded in a homogeneous layer and that careful attention must be paid to other external information about the underground work history. One approach for practical applications might be to get the mean or median of the resistivity values of the medium surrounding the pipe(s), integrated over sections of suitable length, to be used as a tool by the pipe owner.

Thanks to the shallow depth of the required investigations, the capacitive method has a large potential, although development, streamlining and ruggedization of hardware and software would be required before routine application.


## DATA AVAILABILITY STATEMENT


The first version of this manuscript was submitted before data availability was a requirement.


## ACKNOWLEDGEMENTS


The work was done within the framework of the Pipestatus project (<https://www.pipestatus.se/>), which is jointly funded by Vinnova, the pipe owners and the research organizations. In-kind contributions for this study were provided by Lund University, Sorbonne University, Sweden Water Research and the pipe network owners Kraftringen and NSVA. Thanks to the Pipestatus project, and in particular Olle Penttinen.k. We warmly thank the Associate Editor and the two reviewers for their constructive criticism and suggestions.


## ORCID

Simon Rejkjær  <https://orcid.org/0000-0002-1314-0630>

Cécile Finco  <https://orcid.org/0000-0002-2085-3567>

Cyril Schamper  <https://orcid.org/0000-0001-8276-5899>

Fayçal Rejiba  <https://orcid.org/0000-0001-7557-5413>

Alain Tabbagh  <https://orcid.org/0000-0001-7858-8359>

Torleif Dahlin  <https://orcid.org/0000-0001-8431-3263>

## REFERENCES

- Alfano, L.M. (1959) Introduction to the interpretation of resistivity measurements for complicated structural conditions. *Geophysical Prospecting*, 7, 311–368.
- Benderitter, Y., Jolivet, A., Mounir, A. and Tabbagh, A. (1994) Application of the electrostatic quadrupole to sounding in the hectometric depth range. *Journal of Applied Geophysics*, 31, 1–6.
- Boulanger, O. and Chouteau, M. (2005) 3D modelling and sensitivity in DC resistivity using charge density. *Geophysical Prospecting*, 53, 579–617.
- Burton, B.L. and Cannia, J.C. (2011) Capacitively coupled resistivity survey of the levee surrounding the Omaha Public Power District Nebraska City Power Plant: U.S. *Geological Survey Open-File Report*, 2011–1211, 10 p.
- Dabas, M., Camerlynck, C. and Freixas, P. (2000) Simultaneous use of electrostatic quadrupole and GPR in urban context: investigation of the basement of the Cathedral of Girona (Catalunya-Spain). *Geophysics*, 65, 526–532.
- Dahlin, T. and Zhou, B. (2006) Multiple-gradient array measurements for multichannel 2D resistivity imaging. *Near Surface Geophysics*, 4, 113–123.
- Flageul, S., Dabas, M., Thiesson, J., Réjiba, F. and Tabbagh, A. (2013) First in situ tests of a new electrostatic resistivity meter. *Near Surface Geophysics*, 11, 265–273.
- Hesse, A., Andrieux, P., Atya, M., Benech, C., Camerlynck, C., Dabas, M., *et al.* (2002) l'Heptastade d'Alexandrie. *Etudes alexandrines*, 6, IFAO, J.-Y. Empereur (Ed), 191–273.
- Kuras, O., Beamish, D., Meldrum, P.I. and Ogilvy, R.D. (2006) Fundamentals of the capacitive resistivity technique. *Geophysics*, 71, G135–G152.
- Li, Y. and Oldenburg, D.W. (1991) Aspects of charge accumulation in D.C. resistivity experiments. *Geophysical Prospecting*, 39, 803–826.
- Loke, M.H., Acworth, I. and Dahlin, T. (2003) A comparison of smooth and blocky inversion methods in 2-D electrical imaging surveys. *Exploration Geophysics*, 34(3), 182–187.
- Loke, M.H., Chambers, J.E., Rucker, D.F., Kuras, O. and Wilkinson, P.B. (2013) Recent developments in the direct-current geoelectrical imaging methods. *Journal of Applied Geophysics*, 95, 135–156.
- Malm, A., Horstmark, A., Larsson, G., Uusijärvi, J., Meyer, A. and Jansson, E. (2011) *Rörmaterial i Svenska VA-ledningar – egen-skaper och livslängd*. Rapport nr 2011–14, Svenskt Vatten, Stockholm.
- Oldenburg, D.W. and Li, Y. (1999) Estimating depth of investigation in dc resistivity and IP surveys. *Geophysics*, 64, 403–416.
- Roberge, P.R. (2008) *Corrosion Engineering*. McGraw Hill Professional, 754 pp.
- SGU, Geological Survey of Sweden, (2019) Map generator. [Online]. [20 March 2019]. Available from: [http://apps.sgu.se/kartgenerator/maporder\\_en.html](http://apps.sgu.se/kartgenerator/maporder_en.html)
- Spahos, Y. (1979) Calculs sur modèle et rôle du quadripôle en prospection électrique de subsurface. Application à la détection archéologique. Thèse, Université Pierre et Marie Curie, Paris.
- Tabbagh, A., Hesse, A. and Grand, R. (1993) Determination of electrical properties of the ground shallow depth with an electrostatic quadrupole: field trials on archaeological sites. *Geophysical Prospecting*, 41, 579–597.
- Tabbagh, A. and Panissod, C. (2000), 1D complete calculation for electrostatic soundings interpretation. *Geophysical Prospecting*, 48, 511–520.
- Thiesson, J., Tabbagh, A., Dabas, M. and Chevalier, A. (2018) Characterization of buried cables and pipes using electromagnetic induction (EMI) loop-loop frequency domain devices. *Geophysics*, 83, E1–E10.
- Uhlemann, S. and Kuras, O. (2014) Numerical simulations of capacitive resistivity imaging (CRI) measurements. *Near Surface Geophysics*, 12, 523–537.